

ARACNE: An Algorithm for the Reconstruction of Gene Regulatory Networks in a Mammalian Cellular Context

*Adam A. Margolin^{1,2}, Ilya Nemenman^{2,3}, Katia Basso³, Chris Wiggins^{2,4},
Gustavo Stolovitzky⁵, Riccardo Dalla Favera³, Andrea Califano^{1,2,*}*

¹Department of Biomedical Informatics, ²Joint Centers for Systems Biology, ³Institute for Cancer Genetics, ⁴Department of Applied Physics and Applied Mathematics, Columbia University, New York, NY 10032

⁵IBM T.J. Watson Research Center, Yorktown Heights, N.Y. 10598

* To whom correspondence should be addressed:

1130 St. Nicholas Avenue Room 910, New York, NY 10032.

E-mail: califano@c2b2.columbia.edu

Telephone: 212-851-5183, Fax: 212-851-5149

Abbreviations: N_{TP} / N_{FP} , number of true/false positives; N_{TN} / N_{FN} , number of true/false negatives.

ABSTRACT

Elucidating gene regulatory networks is crucial for understanding normal cell physiology and complex pathologic phenotypes. Existing computational methods for the genome-wide “reverse engineering” of such networks have been successful only for lower eukaryotes with simple genomes. Here we present *ARACNE*, a novel algorithm, using microarray expression profiles, specifically designed to scale up to the complexity of regulatory networks in mammalian cells, yet general enough to address a wider range of network deconvolution problems. This method uses an information theoretic approach to eliminate the vast majority of indirect interactions typically inferred by pairwise analysis. We prove that ARACNE reconstructs the network exactly (asymptotically) if the effect of loops in the network topology is negligible, and we show that the algorithm works well in practice, even in the presence of numerous loops and complex topologies. We assess ARACNE’s ability to reconstruct transcriptional regulatory networks using both a realistic synthetic dataset and a microarray dataset from human B cells. On synthetic datasets ARACNE achieves extremely low error rates and significantly outperforms established methods, such as Relevance Networks and Bayesian Networks. Application to the deconvolution of genetic networks in human B cells demonstrates ARACNE’s ability to infer validated transcriptional targets of the c-MYC proto-oncogene.

INTRODUCTION

Biological Background and Significance

Cellular phenotypes are determined by the dynamical activity of large networks of co-regulated genes. Thus dissecting the mechanisms of phenotypic selection requires elucidating the functions of the individual genes in the context of the networks in which they operate. Genome-wide clustering of gene expression profiles [1] provides an important first step towards the identification of such networks. However, the organization of genes into co-regulated clusters is too coarse a representation to identify individual interactions. This is because as biochemical signals travel through cellular networks the expression of many genes that do not directly interact becomes correlated. More generally, as has been appreciated in statistical physics, a long range order (i.e., high correlation among non-directly interacting variables) can easily result from short range interactions [2]. Thus correlations, or *any other* local dependency measure, cannot be used as the only tool for the reconstruction of interaction networks.

Within the last few years a number of sophisticated approaches for the reverse engineering of cellular networks (also called deconvolution) from gene expression data have emerged, such as [3, 4], and many others reviewed in [5]. Their goal is to produce a high-fidelity representation of the cellular network topology as a graph, where genes are represented as vertices and are connected by edges representing direct regulatory interactions. However, all available approaches suffer to various degrees from problems such as overfitting, high computational complexity, reliance on non-realistic network models, or a critical dependency on supplementary data that is only available for simple organisms. These limitations have relegated the successful large-scale application of most methods to relatively simple organisms, such as the yeast *Saccharomyces cerevisiae*, and the genome-wide deconvolution of a mammalian network is yet to be reported. Here we introduce *ARACNE* (Algorithm for the Reconstruction of Accurate Cellular Networks), a novel information-theoretic algorithm for the reverse-engineering of transcriptional networks from microarray data that overcomes some of these critical limitations. ARACNE compares favorably with existing methods and achieves extremely low error rates on a realistic synthetic dataset, and it successfully infers putative transcriptional targets in a mammalian gene network. The algorithm is general enough to deal with a variety of other network reconstruction problems.

Theoretical Background

Several factors have impeded the reliable reconstruction of genome-wide mammalian networks. First, temporal gene expression data is difficult to obtain for higher eukaryotes, and cellular populations harvested from different individuals generally capture random steady states of the underlying biochemical dynamics. This precludes the use of methods that infer temporal associations and thus plausible causal relationships (reviewed in [6]). Only steady-state statistical dependences can be studied, which are not obviously linked to the underlying physical dependency model.

Compounding this constraint, there is no universally accepted definition of statistical dependencies in the multivariate setting [7, 8]. In this work we adopt the definition of [8], which builds on ideas from the Markov networks literature [9]. Briefly, we write the joint

probability distribution (JPD) of the stationary expressions of all genes, $P(\{g_i\})$, $i=1,\dots,N$, as:

$$P(\{g_i\}) = \frac{1}{Z} \exp \left[-\sum_i^N \phi_i(g_i) - \sum_{i,j}^N \phi_{ij}(g_i, g_j) - \sum_{i,j,k}^N \phi_{ijk}(g_i, g_j, g_k) - \dots \right] \equiv e^{-H(\{g_i\})} \quad (1)$$

where N is the number of genes, Z is the *partition function*, $\phi_i(g_i)$ are *potentials*, and $H(\{g_i\})$ is the *Hamiltonian* that defines the system's statistics. Within such a model, we assert that a set of variables interacts *iff* the single potential that depends exclusively on these variables is nonzero. ARACNE aims precisely at identifying which of these potentials are nonzero, and eliminating the others even though their corresponding marginal JPDs may not factorize.

Note that Eq. (1) does not define the potentials uniquely, and additional constraints are needed to avoid the ambiguity. A reasonable approach is to specify $\phi_{...}$ using maximum entropy approximations [8, 10] to $P(g_1, \dots, g_N)$ consistent with known marginals, so that constraining an n -way marginal defines its corresponding potential. We refer the reader to [8] for details.

Approximations of the interaction structure

Since typical microarray sample sizes are relatively small, inferring the exponential number of potential n -way interactions of Eq. (1) is infeasible and a set of simplifying assumptions must be made about the dependency structure. Eq. (1) provides a principled and controlled way to introduce such approximations. The simplest model is one where genes are assumed independent, i.e., $H(\{g_i\}) = \sum_i \phi_i(g_i)$, such that first-order potentials can be evaluated from the marginal probabilities, $P(g_i)$, which are estimated from experimental observations. As more data become available we should be able to reliably estimate higher order marginals and incorporate the corresponding potentials progressively, such that for $M \rightarrow \infty$ (where M is sample set size) the complete form of the JPD is restored. In fact, $M > 100$ is generally sufficient to estimate 2-way marginals in genomics problems, while $P(g_i, g_j, g_k)$ requires about an order of magnitude more samples. Thus the current version of ARACNE truncates Eq. (1) at the pairwise interactions level, $H(\{g_i\}) = \sum_i \phi_i(g_i) + \sum_{i,j} \phi_{ij}(g_i, g_j)$. Within this approximation, all genes for which $\phi_{ij} = 0$ are declared non-interacting. This includes genes that are statistically independent (i.e., $P(g_i, g_j) \approx P(g_i)P(g_j)$), as well as genes that do not interact directly but are statistically dependent due to their interaction with others (i.e., $P(g_i, g_j) \neq P(g_i)P(g_j)$, but $\phi_{ij} = 0$). Since the number of potential pairwise interactions is quadratic in N , discriminating the latter situation is a formidable challenge for all network reconstruction algorithms that rely on statistical associations. However, under certain biologically realistic assumptions about the network topology, the ARACNE algorithm provides a framework to reconstruct two-way interaction networks reliably from a finite number of samples in a computationally feasible time.

ALGORITHM

Within the assumption of a two-way network, all statistical dependencies can be inferred from pairwise marginals, and no higher order analysis is needed. Thus we identify candidate interactions by estimating pairwise gene-gene mutual information (MI), $I(g_i, g_j) \equiv I_{ij}$, an information-theoretic measure of relatedness that is zero *iff* $P(g_i, g_j) = P(g_i)P(g_j)$. We then filter MIs using an appropriate threshold, I_0 , computed for a specific p-value, p_0 , in the null-hypothesis of two independent genes. This step is basically equivalent to the Relevance Networks method [11], and suffers from its critical limitations. In particular, genes separated by one or more intermediaries (indirect relationships) may be highly co-regulated without implying physical interaction, giving rise to false positives.

Thus in its second step, ARACNE removes the vast majority of indirect candidate interactions ($\phi_{ij} = 0$) using a well-known information theoretic property, the data processing inequality (DPI), that has not been previously applied to the reverse engineering of genetic networks.

Mutual Information

Mutual information for a pair of random variables, x and y , is defined as $I(x, y) = S(x) + S(y) - S(x, y)$, where $S(t)$ is the entropy of an arbitrary variable t . For a discrete variable, the *entropy* is $S(t) = -\langle \log p(t_i) \rangle = -\sum_i p(t_i) \log p(t_i)$ where

$p(t_i) = \text{Prob}(t = t_i)$ is the probability of each discrete state (value) of the variable (in this work, logarithms are natural). For continuous variables the entropy is infinite but the MI remains well defined and can be computed by replacing $S(x)$ with the *differential entropy*, which averages the log-probability density rather than the log-mass. Like the more familiar Pearson correlation, MI measures the degree of statistical dependency between two variables. However, while correlation coefficients are not invariant under reparameterizations and may be zero even for manifestly dependent variables, MI is reparameterization invariant and is nonzero *iff* any kind of statistical dependence exists.

MI Estimation: We estimate MI using a computationally efficient Gaussian Kernel estimator [12]. Given a set of two-dimensional measurements, $\vec{z}_i \equiv \{x_i, y_i\}, i = 1 \dots M$, the JPD is approximated as $f(\vec{z}) = 1/M \sum_i h^{-2} G(h^{-1} |\vec{z} - \vec{z}_i|)$, where $G(\dots)$ is the bivariate standard normal density. With $f(x)$ and $f(y)$ being the marginals of $f(\vec{z})$, the MI is:

$$I(\{x_i\}, \{y_i\}) = \frac{1}{M} \sum_i \log \frac{f(x_i, y_i)}{f(x_i) f(y_i)} \quad (2)$$

Since MI is reparameterization invariant, we copula-transform [7] x and y for MI estimation. This decreases the influence of arbitrary transformations involved in microarray data preprocessing and removes the need to consider position-dependent kernel width, h , which might be preferable for the original, non-uniformly distributed data.

For a spatially uniform h , the Gaussian kernel MI estimator is asymptotically unbiased for $M \rightarrow \infty$, as long as $h(M) \rightarrow 0$ and $[h(M)]^2 M \rightarrow \infty$. However, for finite M , the bias strongly depends on $h(M)$ and the correct choice is not universal. Fortunately, ARACNE's performance does not depend directly on the accuracy of the MI estimate, I , but rather on the accuracy of the estimation of MI ranks. For instance, determining if MI is statistically significant requires testing whether $I_{ij} \geq I_0$, where I_0 is the statistical significance threshold. Similarly, the DPI (see below) only requires ranking the MIs.

Producing reliable estimates of the MI ranks is an easier task. From the work on estimation of MI for discrete variables [13], we expect that, for well-sampled marginals and an undersampled joint, the bias is $b \approx b(\bar{I}, h)$ (where the bar denotes the true MI). Thus biases cancel out for similar MI values; the ordering of MI estimates only weakly depends on the choice of h and is stable even when MI itself is uncertain (Figure 1). Thus a single “ensemble best” value of h can be used rather than optimizing the kernel width for each estimate (a computationally intensive operation).

Statistical Threshold for Mutual Information

Since MI is positive semi-definite, its evaluation from random samples gives a positive value even for variables that are, in fact, independent. Therefore, we eliminate all edges for which the null hypothesis of independent genes cannot be ruled out. To this extent, we randomly shuffle the expression of genes across the various microarray profiles, similar to [11], and evaluate the MI for such manifestly independent genes and assign a p-value, p , to an MI threshold, I_0 , by empirically estimating the fraction of the estimates below I_0 . This is done for different sample sizes M and for 10^5 gene pairs so that reliable estimates of $I_0(p)$ are produced up to $p = 10^{-4}$. Extrapolation to smaller p-values is done using $p(I \geq I_0 | \bar{I} = 0) \propto e^{-\alpha M I_0}$, where the parameter α is fitted from the data. This formula is based on the intuition of the large deviation theory [14], which for discrete data and unbiased estimators suggests $p(I \geq I_0 | \bar{I} = 0) \propto e^{-M I_0}$. As MI in the continuous case can be estimated by finely discretizing the variables, a similar result should hold, and α accounts for possible biases of the estimator at fixed h . This produces an excellent agreement with numerical experiments*.

Data Processing Inequality

The DPI [14] states that if genes g_1 and g_3 interact only through a third gene, g_2 , [i.e., if the interaction network is $g_1 \leftrightarrow \dots \leftrightarrow g_2 \leftrightarrow \dots \leftrightarrow g_3$ and no alternative path exists between g_1 and g_3], then

$$I(g_1, g_3) \leq \min[I(g_1, g_2); I(g_2, g_3)]. \quad (3)$$

Thus the least of the three MIs can come from indirect interactions only, and checking against the DPI may identify those gene pairs for which $\phi_{ij} = 0$ even though $P(g_i, g_j) \neq P(g_i)P(g_j)$. Correspondingly, ARACNE starts with a network graph where

* See supporting materials

each $I_{ij} > I_0$ is represented by an edge (ij) . The algorithm then examines each gene triplet for which all three MIs are greater than I_0 and removes the edge with the smallest value. Each triplet is analyzed irrespectively of whether its edges have been marked for removal by prior DPI applications to different triplets. Thus the network reconstructed by the algorithm is independent of the order in which the triplets are examined.

Theorem 1[†]. If MIs can be estimated with no errors, then ARACNE reconstructs the underlying interaction network exactly, provided this network is a tree and has only pairwise interactions.

However, unlike standard tree reconstruction methods (e.g. Chow and Liu [15]), ARACNE is not limited to trees and can produce complicated, loopy structures. In fact, because of the following two theorems, ARACNE can be viewed as a natural generalization of the Chow-Liu algorithm which overcomes the biologically-unrealistic tree assumption of the latter.

Theorem 2. The Chow-Liu (CL) maximum mutual information tree is a subnetwork of the network reconstructed by ARACNE.

Theorem 3. Let π_{ik} be the set of nodes forming the shortest path in the network between nodes i and k . Then, if MIs can be estimated without errors, ARACNE reconstructs an interaction network without false positives edges, provided: (a) the network consists only of pairwise interactions, (b) for each $j \in \pi_{ik}$, $I_{ij} \geq I_{ik}$. Further, ARACNE does not produce any false negatives, and the network reconstruction is exact *iff* (c) for each directly connected pair (ij) and for any other node k , we have $I_{ij} \geq \min(I_{jk}, I_{ik})$.

Note that tree networks satisfy all conditions of Theorem 3, while loopy topologies may or may not. In particular, networks with three-gene loops definitely violate (c) [but may still satisfy (a) and (b)], and *every* such loop will be opened along the weakest edge. For a tree, there is a unique path that connects two nodes. Similarly, for networks that satisfy (a) and (b), the shortest path dominates inter-node information transfer. We call these networks *locally tree-like*. In other words, an interaction is retained by ARACNE if and only if there exist no alternate paths, via one or more intermediaries or branches on the network graph, which are a better explanation for the information exchange between two genes. Since biochemical dynamics is inherently stochastic, statistical interactions over more than a few separating edges are generically weak. Thus we believe that the local tree assumption is biologically realistic, and we expect ARACNE to produce low false positive rates in practice.

Finally, to minimize the impact of potential MI estimation errors, a tolerance, τ , may be introduced such that the DPI inequalities become of the form $I_{ij} \leq I_{ik}(1 - \tau)$, and close values of MI are not pruned. Using such non-zero tolerance leads to persistence of some 3-gene loops. For low values of τ (<15%) a reasonable tradeoff between true positives and false positives is achieved*.

Algorithmic Complexity

[†] Proofs of all theorems can be found in the supporting materials.

Because for a network of N genes there are at most N choose 3 gene triplets, ARACNE's complexity is $O(N^3 + N^2M^2)$, where M is the number of samples and N is the number of genes. The first term relates to the DPI analysis and the second to the mutual information estimation. This compares favorably with optimization methods that must explore an exponential search space. In practice, the DPI is applied to a small subset of triplets for which all three edges survive the mutual information thresholding. Therefore, for large M , the computationally intensive part is generally associated with the second term (computing mutual information), which scales as $O(N^2M^2)$. As a result, ARACNE can efficiently analyze networks with tens of thousands of genes.

RESULTS

We study ARACNE's performance in reconstructing a class of synthetic networks proposed by [16] and a human B lymphocyte genetic network from gene expressions profile data. ARACNE's performance is compared against Relevance Networks (RNs) and Bayesian Networks (BNs). RNs are important to characterize the improvement associated with the introduction of the DPI, while BNs have emerged as some of the most widely used reverse engineering methods and provide an ideal comparative benchmark.

Comparative Algorithms

A *Bayesian Network* is a representation of a JPD as a directed acyclic graph (DAG) whose vertices correspond to random variables $\{X_1, \dots, X_n\}$, and whose edges correspond to parent-child dependencies among variables; see [9] for an introduction and [17] for a more recent tutorial. In this work, BN results were produced using the software from Nir Friedman's Computational Biology group [18], which is among the best implementations of the method. We searched the graph space using the greedy hill climbing algorithm with random restarts (other search methods were tested with similar results).

Relevance Networks [11] compute mutual information for all gene pairs in a microarray dataset and infer that two genes are biologically related if they have the MI above a certain threshold. This approach is basically equivalent to the first step in the ARACNE algorithm (i.e. without the DPI).

Synthetic Networks

Networks Specification: We benchmark the three algorithms using synthetic transcriptional networks proposed by Mendes *et al.* [16] as a platform for comparison of reverse-engineering algorithms. These networks consist of 100 genes and 200 interactions organized either in an Erdős-Rényi (random network) [19] or a scale-free [20] topology. In the former, each vertex of a graph is equally likely to be connected to any other vertex; in the latter, the distribution of the number of connections, k , associated with each vertex follows a power law, $p(k) \sim k^{-\gamma}$ with $\gamma > 0$, and large interactions hubs are present. Many real biological networks appear to exhibit such structure [21].

The Mendes models use a multiplicative Hill dynamics to approximate transcriptional interactions:

$$\frac{dx_i}{dt} = a_i \prod_{j=1}^{N_I} \frac{IK_j^{n_j}}{IK_j^{n_j} + I_j^{n_j}} \prod_{l=1}^{N_A} 1 + \frac{A_l^{m_l}}{AK_l^{m_l} + A_l^{m_l}} - b_i x_i, \quad (4)$$

where x_i is the concentration (expression) of the i -th gene, N_I and N_A are the number of upstream inhibitors and activators respectively, and their concentrations are I_j and A_l . All other parameters are specified in [16].

We obtain synthetic expression values of each gene x_i in each microarray M_k by simulating its dynamics until the system relaxes to a steady state $\dot{x}_i \approx 0$. Prior to each simulation, the efficiency of synthesis and degradation reactions are varied by setting $a_i = \lambda_{k,i} \bar{a}_i$ and $b_i = \gamma_{k,i} \bar{b}_i$, where \bar{a}_i and \bar{b}_i are the original constant values of the parameters, and $\lambda_{k,i}, \gamma_{k,i}$ are random variables uniformly distributed in [0.0, 2.0]. Note that $\lambda_{k,i} \sim 0.0$ corresponds to a gene knock-out, while $\lambda_{k,i} \sim 2.0$ is a 2-fold increase in the synthesis rate. This parameter randomization models the sampling of a population of distinct cellular phenotypes at random time points (at or close to equilibrium), as is the case for the B cell experiments described later, where the efficiency of individual biochemical reactions may be different from assay to assay due to differences in temperature, nutrients, genetic mutations, etc. Under such perturbations, the relationships between simulated genes across all experiments appear consistent with those observed in real experiments from the B cells.

Performance metrics: Since genetic networks are sparse potential false positives far exceed potential true positives. Thus *specificity*, $N_{TN} / (N_{FP} + N_{TN})$, which is typically used in ROC analysis, is inappropriate as even small deviation from a value of 1 will result in large false positive numbers. Therefore, we choose two closely related metrics, *precision* and *recall*. Recall, $N_{TP} / (N_{TP} + N_{FN})$, indicates the fraction of true interactions correctly inferred by the algorithm, while precision, $N_{TP} / (N_{TP} + N_{FP})$, measures the fraction of true interactions among all inferred ones. Note that precision corresponds to the expected success rate in the experimental validation of predicted interactions. Performance will thus be assessed using Precision-Recall Curves (PRCs). PRCs for ARACNE and RNs are generated by adjusting the p-value or, equivalently, the MI threshold. ARACNE's PRC does not extend to 100% recall since the DPI eliminates some interactions even at $p_0 = 1$. To reach the 100% recall, the DPI tolerance, τ , can be adjusted until ARACNE's PRC degenerates into that of RNs. For BNs, the adjustable parameter is the Dirichlet pseudocount, and, again, we observe that the maximum recall never reaches 100%.

Performance Evaluation: As shown in **Figure 2**, values of precision and recall for ARACNE are consistently better than those for the other methods. That is, for any reasonable precision (i.e. $> 40\%$), ARACNE has a significantly higher recall than the other methods, and its precision reaches $\sim 100\%$ at significant recall levels. For large p-values, ARACNE begins to rapidly increase the number of false positives without a corresponding increase in true positives (the right tail of ARACNE's PRC). This is likely

because as non-statistically significant MI values are accepted, random fluctuations may arbitrarily change the MI rank so that the DPI removes interactions at random. We note that the inflection of the PRC for ARACNE starts at $p_0 \sim 10^{-4}$, exactly where we would expect the algorithm to begin inferring large numbers of non-statistically significant interactions for a network of this size. This suggests that a sensible value for the MI threshold, producing a near optimal result, can be selected a-priori using a Bonferroni-corrected p-value based on the number of potential network interactions.

ARACNE's high performance can be better understood by analyzing the distribution of MIs as a function of the length of the shortest path connecting each gene pair (degree of connectivity). ARACNE depends on MI being enriched for directly interacting genes and decreasing rapidly with this distance. Figure 3 demonstrates these properties for our simulated datasets. There is no unique choice for the MI threshold that separates directly and indirectly interacting genes, and methods such as RNs that attempt to use a single threshold will either recover many indirect connections or miss a substantial number of direct ones. However, since mutual information decreases rapidly as signals travel over the network, the DPI effectively eliminates indirect interactions whose JPD does not factorize. For all tested synthetic microarray sizes and both network topologies, ARACNE recovers far more true connections and far fewer false connections than the other methods (**Table 1**). Remarkably, in all cases, application of the DPI eliminates almost all indirect candidate interactions inferred by Relevance Networks at the expense of very few true interactions. We note that since ARACNE's performance degrades as the local topology deviates significantly from a tree, it performs slightly better on Erdős-Rényi than on scale-free topologies, for which small loops are much more common. Another challenge in reconstructing the scale-free topology derives from the presence of large hubs with high in-degrees, which obscure MI estimation. However, ARACNE still performs extremely well even on scale-free topologies because signals in this network decorrelate rather quickly, so the statistical properties of a tree-like structure are locally preserved even in the presence of relatively tight loops (see Theorem 3).

In summary, ARACNE appears to (a) achieve very high precision and substantial recall, even for few data points (125), (b) allow an optimal choice of the parameters h (Gaussian Kernel width) (**Figure 1**) and I_0 (statistical threshold), (c) to be quite stable with respect to the choice of parameters, and (d) to produce robust reconstruction of complex topologies containing many loops.

Human B Cells

Although large gene expression datasets such as those derived from systematic perturbations to simple organisms (e.g., [22]) are not easily obtained for mammalian cells, we suggest that an equivalent dynamic richness can be efficiently achieved by using a significant set of naturally occurring and experimentally generated phenotypic variations of a given cell type. To this end, we have assembled an expression profile dataset consisting of about 340 B lymphocytes derived from normal, tumor-related, and experimentally manipulated populations (for an extensive description see [23])

This dataset was deconvoluted using ARACNE to generate a B cell specific regulatory network consisting of approximately 129,000 interactions. Since the c-MYC proto-oncogene emerges as one of the top 5% largest cellular hubs in the complete network and

is extensively characterized in the literature as a transcription factor, we performed a first validation of the overall network quality by comparing its interactions inferred by our method with those previously identified by biochemical methods. The *in silico* generated network is highly enriched in known c-MYC targets; 29 out of 56 (51.8%) genes predicted to be first neighbors were either previously reported in the literature or biochemically validated in our labs as c-MYC targets, as reported in [24]. This is statistically significant ($P = 2.9 \times 10^{-23}$ by χ^2 test) with respect to the expected 11% of background c-MYC targets among randomly selected genes [25]. In addition, known c-MYC target genes were significantly more enriched among first neighbors than among second neighbors (51.8% vs. 19.4%), indicating that ARACNE is effective at separating direct regulatory interactions from indirect ones.

DISCUSSION

ARACNE, which is motivated by statistical mechanics and based on an information theoretic approach, provides a provably exact network reconstruction under a controlled set of approximations. While we have shown that these approximations are reasonable even for complex mammalian gene networks, they may cause the algorithm to fail for some control structures. First, ARACNE will open all three-gene loops along the weakest interaction (although some may be preserved when a non-zero DPI threshold is used), and improvements to the algorithm must be investigated to address this condition. Second, by truncating Eq. (1) at the pairwise interactions, ARACNE will not infer statistical dependencies that are not expressed as pairwise interaction potentials (such as an XOR Boolean table for which MI between any gene pair is zero). By expanding Eq. (1) to include third and higher order potentials our formulation, in principle, can be extended to distinguish higher order interactions as well. However, we note that in practice (i.e., biochemically) it is difficult to produce *only* higher order interactions without introducing some lower order dependencies, and truncation of the Hamiltonian is not likely to produce serious systematic errors in identifying interactions between gene pairs. In fact, the Mendes networks contain higher order interactions, but corresponding pairwise ones are effectively recovered instead. Another limitation of ARACNE is the inability to infer edge directionality, and we intend to investigate a two-tier approach in which first adirectional gene interactions are inferred, and then edge directionality is assessed via regression algorithms or specific biochemical perturbations. The synthetic networks platform we have implemented will be useful to test extensions of the algorithm to address the above-described limitations. It will also help assess the ability of ARACNE to infer more complex *cis*-regulatory and non-transcriptional interactions and to evaluate the effects of factors such as reaction and measurement noise, as well as the limited availability of monitored molecular species.

ARACNE overcomes several limitations that have impeded the application of previous methods to the genome-wide analysis of mammalian networks. It has a low computational complexity, does not require discretization of the expression levels, and does not rely on unrealistic network model or *a priori* assumptions. The algorithm can be applied to arbitrarily complex networks of transcriptional, or any other, interactions without reliance on heuristic search procedures. Thus ARACNE is well suited for mammalian gene regulatory networks which are characterized by a complex topology, do

not benefit from well-defined supplemental data (such as comprehensive protein interaction databases available for yeast), and are more difficult to manipulate experimentally, substantially hindering the acquisition of data to which time-series based methods can be applied. There are currently no other examples of a genome-wide mammalian network inferred from microarray expression profiles. As suggested by the inference of putative transcriptional interactions in human B cells, ARACNE shows significant promise in an area that has challenged reverse engineering algorithms.

FIGURE LEGENDS AND TABLES

Figure 1

Performance evaluation for varying Gaussian kernel widths. **(Left axis)** The mean absolute percent error in estimating mutual information for bivariate normal densities is compared to the percent of errors in ranking the relative mutual information values for randomly sampled pairs for which the distribution with the lower true MI value is between 70% and 99% of the distribution with the higher value. MI estimation error (dashed blue line) is highly sensitive to the choice of Gaussian kernel width used by the estimator and grows rapidly for non-optimal parameter choices. However, due to similar bias for distributions with close MI values, the error in ranking pairs of MIs (dashdot blue line) is much less sensitive to the choice of this parameter. These averages were produced using samples from 1,000 bivariate normal densities with a random uniformly distributed correlation coefficient $\rho \in [0.1, 0.9]$, such that $\bar{I} = -\frac{1}{2} \log(1 - \rho^2)$. This results in a distribution of MI values that closely resembles that of the real microarray data. **(Right axis)** The total number of inferred errors ($N_{FP} + N_{FN}$) in reconstructing the Mendes networks (see **Synthetic Networks**) is stable with respect to choice of estimator kernel width, validating the observation that rankings of MIs are more stable than the MI estimates with respect to changes in this parameter. The choice of kernel width for each number of samples that minimizes the mean absolute MI estimation error for bivariate Gaussian densities (indicated with diamonds) yields optimal or near optimal reconstruction of this network for all samples sizes. Results are calculated for a statistical significance threshold of 10^{-4} and a synthetic microarray size of 1,000 for the scale-free network topology.

Figure 2

Precision vs. Recall for 1,000 samples generated from the Mendes network. **(a)** Erdös-Rényi network topology. **(b)** Scale-free topology. ARACNE's PRCs are consistently better than those of the other algorithms, and the precision reaches $\sim 100\%$ while maintaining high recall. Points on the PRCs for ARACNE and RNs corresponding to $p_0 = 10^{-4}$ (the value yielding < 0.5 expected false positives for 4,950 potential interactions) are indicated with arrows.

Figure 3

Distribution of mutual information for different lengths of the shortest path between genes for the scale-free topology. Here we plot the log of the empirical probability that MI for a given separation between genes is above some value (in nats) marked on the horizontal axis. High MI values are significantly more probable for closer genes. Statistical significance threshold of 10^{-4} for the background MI distribution, corresponding to $I_0 = 0.0175$ nats, is marked on the graph. As shown, this threshold retains a large number of indirect candidate interactions, and there is no threshold that would be able to separate indirect and direct interactions; a threshold that eliminates most

of the former (red arrows) also eliminates the majority of the latter. This severely degrades performance of RNs. **(Inset)** Expanded log-log view of the MI distribution for 934 gene pairs with 3 or more intermediaries and the background distribution computed by Monte Carlo. The curves are virtually indistinguishable, indicating that the background distribution can be used to obtain reliable estimates of statistical significance thresholds for filtering genes with higher degrees of connectivity. Similar results apply for the Erdős-Rényi topology*.

Table 1

Erdős-Rényi Topology

Num samples	ARACNE		Relevance Networks		DPI Sensitivity	DPI Precision	Bayesian Networks	
	N_{TP}	N_{FP}	N_{TP}	N_{FP}			N_{TP}	N_{FP}
1000	128.00	1.33	143.33	462.67	99.71%	96.78%	50.00	32.33
750	124.33	2.67	139.33	411.00	99.35%	96.46%	45.33	31.00
500	119.00	1.67	130.67	311.33	99.46%	96.37%	41.00	29.00
250	101.00	4.67	110.00	182.33	97.44%	95.18%	24.67	25.33
125	81.00	4.67	84.67	95.00	95.09%	96.10%	5.33	19.00

Scale-Free Topology

Num samples	ARACNE		Relevance Networks		DPI Sensitivity	DPI Precision	Bayesian Networks	
	N_{TP}	N_{FP}	N_{TP}	N_{FP}			N_{TP}	N_{FP}
1000	97.67	2.33	113.33	234.00	99.00%	93.67%	38.67	17.00
750	90.67	3.33	103.00	200.00	98.33%	94.10%	33.33	15.33
500	80.33	5.33	91.67	154.67	96.55%	92.95%	27.00	13.33
250	63.33	7.67	70.00	80.00	90.42%	91.56%	9.00	9.67
125	46.33	3.67	48.00	49.67	92.62%	96.50%	4.00	6.00

Recovery for varying numbers of samples generated from the Mendes networks, which contain an average of ~ 194 true interactions after self-loops and bidirectional edges are eliminated. For all sample sizes ARACNE efficiently eliminates almost all false candidate interactions inferred by RNs, as indicated by the DPI sensitivity (calculated as the percent of false positives eliminated by the DPI), with minimal reduction in true positives, as indicated by the DPI precision (calculated as the percent of false positives removed out of the total number of edges removed by the DPI). Moreover, as the sample size decreases, the number of true connections inferred by ARACNE decays gracefully while the number of false positives remains very low, whereas the performance of Bayesian Networks degrades rapidly for smaller sample sizes as the conditional probability tables become very sparsely populated. Results are calculated using a p-value

of 10^{-4} for ARACNE and Relevance Networks, yielding < 0.5 expected false positives for 4,950 potential interactions, and using a Dirichlet prior with equivalent sample size of one for Bayesian Networks [26]. Results are averaged over three network configurations for each topology.

1. Eisen, M.B., et al., *Cluster analysis and display of genome-wide expression patterns*. Proc Natl Acad Sci U S A, 1998. **95**(25): p. 14863-8.
2. Ma, S.-K., *Statistical mechanics*. 1985, Singapore: World Scientific.
3. Gardner, T.S., et al., *Inferring genetic networks and identifying compound mode of action via expression profiling*. Science, 2003. **301**(5629): p. 102-5.
4. Friedman, N., *Inferring cellular networks using probabilistic graphical models*. Science, 2004. **303**(5659): p. 799-805.
5. van Someren, E.P., et al., *Genetic network modeling*. Pharmacogenomics, 2002. **3**(4): p. 507-25.
6. Wiggins, C. and I. Nemenman, *Process pathway inference via time series analysis*. Experimental Mechanics, 2003. **43**(3): p. 361--370.
7. Joe, H., *Multivariate models and dependence concepts*. 1997, Boca Raton, FL: Chapman & Hall.
8. Nemenman, I., *Information theory, multivariate dependence, and genetic network inference*, in *Tech. Rep. NSF-KITP-04-54, KITP, UCSB*. 2004, arXiv: q-bio/0406015.
9. Pearl, J., *Probabilistic reasoning in intelligent systems: networks of plausible inference*. 1988, San Francisco, CA: Morgan Kaufmann Publishers, Inc.
10. Janes, E.T., *Information theory and statistical mechanics*. Phys. Rev., 1957. **106**: p. 620--630.
11. Butte, A.J. and I.S. Kohane, *Mutual information relevance networks: functional genomic clustering using pairwise entropy measurements*. Pac Symp Biocomput, 2000: p. 418-29.
12. Beirlant, J., et al., *Nonparametric entropy estimation: An overview*. Int. J. Math. Stat. Sci., 1997. **6**(1): p. 17-39.
13. Strong, S.P., et al., *Entropy and information in neural spike trains*. Phys. Rev. Lett., 1998. **80**(1): p. 197-200.
14. Cover, T.M. and J.A. Thomas, *Elements of Information Theory*. 1991, New York: John Wiley & Sons.
15. Chow, C.K. and C.N. Liu, *Approximating discrete probability distributions with dependence trees*. IEEE Trans. Inf. Thy, 1968. **IT-14**(3): p. 462-467.
16. Mendes, P., W. Sha, and K. Ye, *Artificial gene networks for objective comparison of analysis algorithms*. Bioinformatics, 2003. **19 Suppl 2**: p. II122-II129.
17. Heckerman, D., *A Tutorial on Learning with Bayesian Networks*. 1996, Microsoft Research.
18. Friedman, N. and G. Elidan, *LibB 2.1*, <http://www.cs.huji.ac.il/labs/compbio/LibB/>. 2004.
19. Erdos, P. and A. Renyi, *On Random Graphs*. Publ. Math. Debrecen, 1959. **6**: p. 290-297.

20. Barabasi, A.L. and R. Albert, *Emergence of scaling in random networks*. Science, 1999. **286**(5439): p. 509-12.
21. Newman, M.E.J., *The Structure and Function of Complex Networks*. SIAM Review, 2003. **45**(2): p. 167-256.
22. Ideker, T., et al., *Integrated genomic and proteomic analyses of a systematically perturbed metabolic network*. Science, 2001. **292**(5518): p. 929-34.
23. Klein, U., et al., *Gene expression profiling of B cell chronic lymphocytic leukemia reveals a homogeneous phenotype related to memory B cells*. J Exp Med, 2001. **194**(11): p. 1625-38.
24. Basso, K., et al., *Reverse engineering of regulatory networks in human B cells*. Nat Genet, *Submitted*.
25. Fernandez, P.C., et al., *Genomic targets of the human c-Myc protein*. Genes Dev, 2003. **17**(9): p. 1115-29.
26. Hartemink, A.J., et al., *Using graphical models and genomic expression data to statistically validate models of genetic regulatory networks*. Pac Symp Biocomput, 2001: p. 422-33.

SUPPORTING MATERIALS

Proofs of Theorems

Theorem 1. If MIs can be estimated with no errors, then ARACNE reconstructs the underlying interaction network exactly, provided this network is a tree and has only pairwise interactions.

Proof of Theorem 1. First, notice that for every pair of nodes i and k not connected by a true direct interaction there is at least one other node j that separates them on the network tree. Applying the DPI to the (ijk) triplet leads to removal of the (ik) edge. Thus only true edges survive. Similarly, every removed edge is not present in the true network. Consider some (ijk) triplet. One of these nodes, say j , may separate the other two. In this case the removed edge (ik) is clearly not in the true tree. Alternatively, there may be no separating node, and one may be able to move between any pair in the triplet without going through the third one. In this case none of the three edges is in the true graph, and any edge the DPI removes is fictitious. Thus all removed edges are indirect, while all remaining edges are factual. The network is reconstructed exactly.

Theorem 2. Chow-Liu (CL) maximum mutual information tree is a subnetwork of the network reconstructed by ARACNE.

Proof of Theorem 2. We notice that, without a loss of generality, we can assume that the Chow-Liu tree and the ARACNE construction span all the nodes of the network. If this is not the case, that is, a few connected clusters exist (separated by edges with zero MI), then for the purpose of this theorem we can complete CL and ARACNE structures by the same edges with zero MI without formation of additional loops, till they become spanning. Now suppose that the theorem is false and there exists an edge (ij) that belongs to the (completed) CL tree, but does not belong to the ARACNE reconstruction. Since the CL construct is a tree, this edge separates it into two separate trees T_i and T_j that contain the i 'th and the j 'th nodes respectively. Since ARACNE has removed the (ij) link, there exists a node k , for which $\min(I_{ik}, I_{jk}) > I_{ij}$. Without a loss of generality, let k be in T_i . Then replacing the (ij) edge in the Chow-Liu tree by the (jk) edge will form no loops and will preserve the tree structure. This will increase the total MI of the CL reconstruction by $I_{jk} - I_{ij} > 0$. Thus the original tree is not the maximum MI tree. We arrive at a contradiction, which proves the theorem.

Theorem 3. Let π_{ik} be the set of nodes forming the shortest path in the network between nodes i and k . Then, if MIs can be estimated without errors, ARACNE reconstructs an interaction network without false positives edges, provided: (a) the network consists only of pairwise interactions, (b) for each $j \in \pi_{ik}$, $I_{ij} \geq I_{ik}$. Further, ARACNE does not produce any false negatives, and the network reconstruction is exact *iff* (c) for each directly connected pair (ij) and for any other node k , we have $I_{ij} \geq \min(I_{jk}, I_{ik})$.

Proof of Theorem 3. To prove the absence of false positives, we notice that, for every candidate edge (ik) that is not actually in the network, there is at least one node j , such that $j \in \pi_{ik}$. Applying DPI to the (ijk) triplet will remove the (ik) edge. Further, we notice

that if (c) is satisfied, then any application of DPI will not remove a true edge. However, if (c) does not hold, a true edge will be removed. This completes the proof.

Relations to Graphical Models and Statistical Physics

The definition of dependencies employed in the paper, which is based on the presence of a potential that couples interacting genes in the JPD,

$$P(\{g_i\}) = \frac{1}{Z} \exp \left[-\sum_i \phi_i(g_i) - \sum_{i,j} \phi_{ij}(g_i, g_j) - \sum_{i,j,k} \phi_{ijk}(g_i, g_j, g_k) - \dots \right] \equiv e^{-H(\{g_i\})}, \quad (5)$$

is similar to that used in the theory of graphical models, specifically Markov Networks (MNs) [1]. However, even though there are some dissenting formulations (e.g., [2]), the usual implementation of MNs [1] is built using the notion of conditional (in)dependence. In this context it is impossible to distinguish, for example, a clique of three genes that are fully coupled by three pairwise interactions from the same genes coupled by a third order dependence, and also from a combination of both cases. Because of this, many authors use a convention that if a higher order potential $\phi_{...}$ is present in Equation 1, then all lower order potentials that depend only on a subset of the genes coupled by $\phi_{...}$ are incorporated into it. In contrast, the definition of [3], followed in this paper, aims at discriminating interaction orders. Thus, in our case, a three gene pairwise loop is distinct from a three-way interaction. In fact, extensions of ARACNE to deal with the latter have been developed [4], while the former still requires work.

As is understood in the graphical models literature, the formulation of Equation 1 resembles some statistical mechanics problems, specifically spin glasses on random networks [2, 5], particularly if the g_i are binary (such discretization of expression levels is a common technique to deal with undersampling). In this case, the genes are the Ising spins, and truncations to the first, second, or the third order potentials are steps towards the mean field, Bethe, and Kikuchi variational approximations [2, 6-8]. An important distinction is that in statistical physics one searches for $\tilde{P}(\{g_i\})$, a variational approximation to the true JPD, $P(\{g_i\})$, that minimizes $D_{KL}(\tilde{P} \| P) \equiv \langle \log \tilde{P} / P \rangle_{\tilde{P}}$ within a given class of \tilde{P} , while the definition of [3] is equivalent to minimizing $D_{KL}(P \| \tilde{P})$. This is because statistical physics solves a direct problem – calculating various spin statistics given an interaction network. In particular, low order marginals $P_{...}$ are unknown and cannot be used in averaging. On the other hand, we are here solving the inverse problem – reconstructing the network given the known true marginal distributions.

ARACNE, which truncates Equation 1 at the second order potentials, is an analog of the Bethe approximation for the direct problem. Just like this approximation and the associated belief propagation algorithm [1, 9], ARACNE may fail for loopy topologies. It is, therefore, appealing that, for locally tree-like networks, the algorithm still works well, paralleling the corresponding discussion in statistical physics [9].

1. Pearl, J., *Probabilistic reasoning in intelligent systems: networks of plausible inference*. 1988, San Francisco, CA: Morgan Kaufmann Publishers, Inc.
2. Yedidia, J., *An idiosyncratic journey beyond mean field theory*, in *Advanced Mean Field Methods: Theory and Practice*, M. Opper and D. Saad, Editors. 2001, MIT Press: Cambridge, MA.
3. Nemenman, I., *Information theory, multivariate dependence, and genetic network inference*, in *Tech. Rep. NSF-KITP-04-54, KITP, UCSB*. 2004, arXiv: q-bio/0406015.
4. Wang, K., et al., *Conditional Network Analysis Identifies Candidate Regulator Genes in Human B Cells*. E-print q-bio.MN//0411003, 2004.
5. Mezard, M. and G. Parizi, *The Bethe lattice spin glass revisited*. *Eur. Phys. J. B*, 2001. **20**: p. 217.
6. Bethe, H., *Statistical Theory of Superlattices*. *Proc. Roy. Soc. London A*, 1935. **150**: p. 552.
7. Kikuchi, R., *A Theory of Cooperative Phenomena*. *Phys. Rev.*, 1951. **81**: p. 988.
8. Opper, M. and O. Winther, *From naive mean field theory to the TAP equations*, in *Advanced mean field methods: theory and practice*, M. Opper and D. Saad, Editors. 2001, MIT Press: Cambridge, MA.
9. Yedidia, J.S., W.T. Freeman, and Y. Weiss, *Generalized Belief Propagation*. Advances in Neural Information Processing Systems (NIPS), 2001. **13**: p. 689-695.

SUPPORTING FIGURE LEGENDS

Figure 5

Examples of the Data Processing Inequality.

(a) g_1 , g_2 , and g_3 , are connected in a linear chain relationship. Although all six gene pairs will likely have enriched mutual information, the DPI will infer the most likely path of information flow. For example, $g_1 \leftrightarrow g_3$ will be eliminated because $I(g_1, g_2) > I(g_1, g_3)$ and $I(g_2, g_3) > I(g_1, g_3)$. $g_2 \leftrightarrow g_4$ will be eliminated because $I(g_2, g_3) > I(g_2, g_4)$ and $I(g_3, g_4) > I(g_2, g_4)$. $g_1 \leftrightarrow g_4$ will be eliminated in two ways: first, because $I(g_1, g_2) > I(g_1, g_4)$ and $I(g_2, g_4) > I(g_1, g_4)$, and then because $I(g_1, g_3) > I(g_1, g_4)$ and $I(g_3, g_4) > I(g_1, g_4)$. **(b)** If the underlying interactions form a tree (and MI can be measured without errors), ARACNE will reconstruct the network exactly by removing all false candidate interactions (dashed blue lines) and retaining all true interactions (solid black lines).

Figure 6

The number of inferred errors, $N_{FP} + N_{FN}$, are plotted as a function of the DPI tolerance, τ , for **(a)** the Erdős-Rényi and **(b)** the scale-free topologies. Raising τ to a value of 0.2 results in a modest increase in false positives, while larger values of τ produce a much sharper increase. Therefore, a moderate choice for the tolerance can help elucidate

additional interactions without introducing an excessive number of false positives. Results are calculated for a statistical significance threshold of 10^{-4} and a synthetic microarray size of 1,000.

Figure 7

Topology of the 100 gene regulatory networks proposed by Mendes. Blue/red edges correspond to activation/inhibition. For the Erdős-Rényi topology **(a)** each gene is equally likely to be connected to every other gene, while the scale-free topology **(b)** is characterized by large interaction hubs with many connections.

Figure 8

Distribution of mutual information for different lengths of the shortest path between genes for the Erdős-Rényi topology. Red and black arrows are explained in the legend of Figure 3. Since there are no large in-degree hubs, decorrelation is slower than for the scale-free network, and MI statistics even for fifth neighbors is still distinguishable from the background.

Figures

Figure 1.

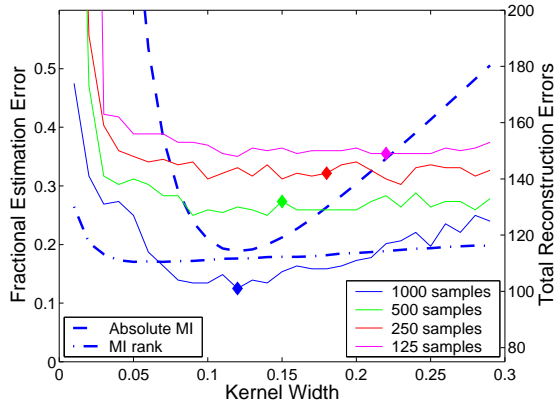


Figure 2.

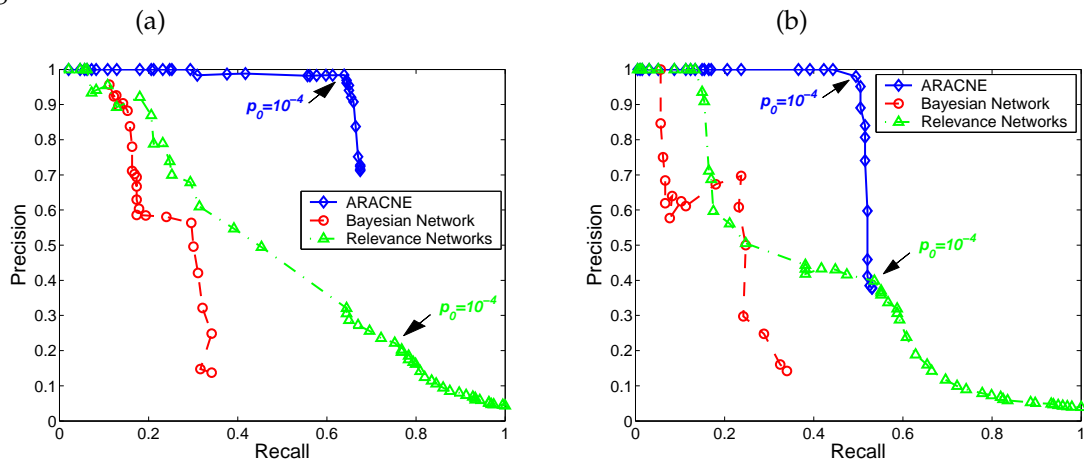


Figure 3.

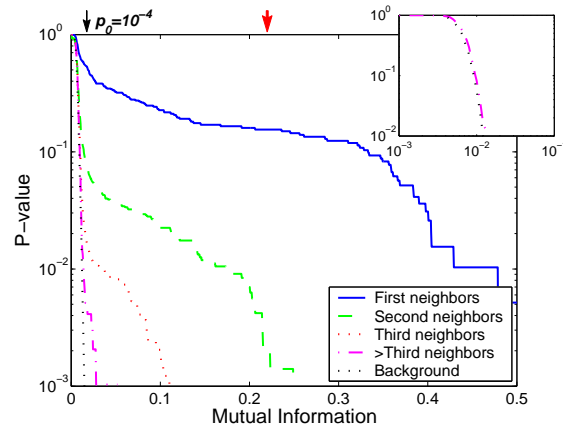


Figure 4.

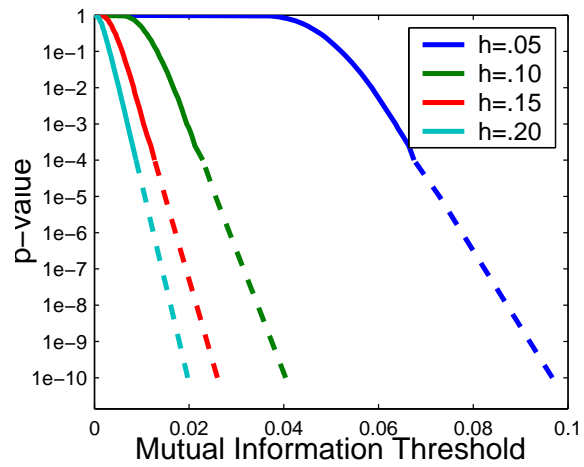


Figure 5.

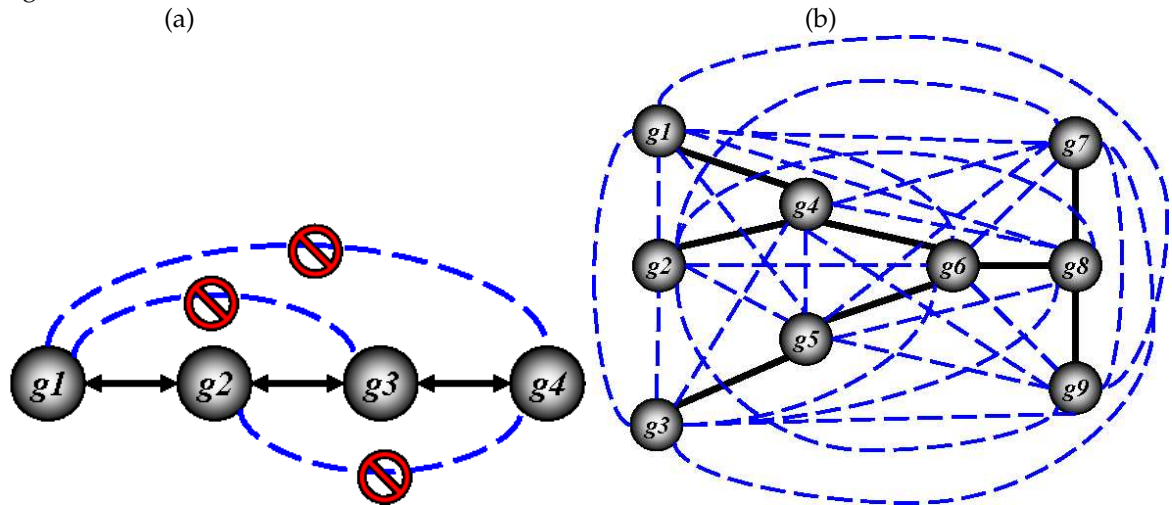


Figure 6.

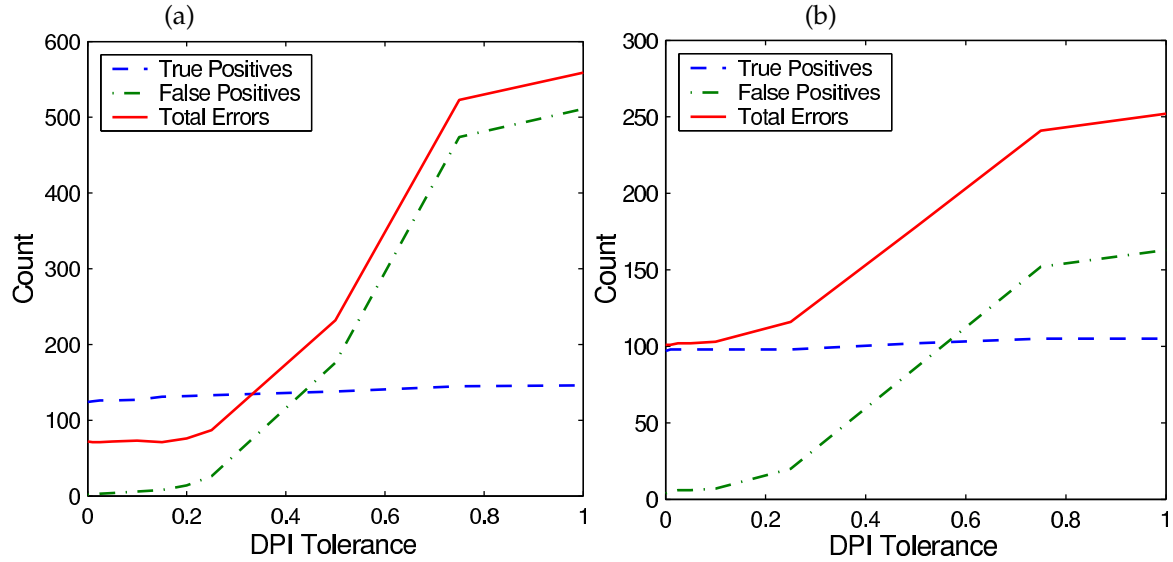


Figure 7.

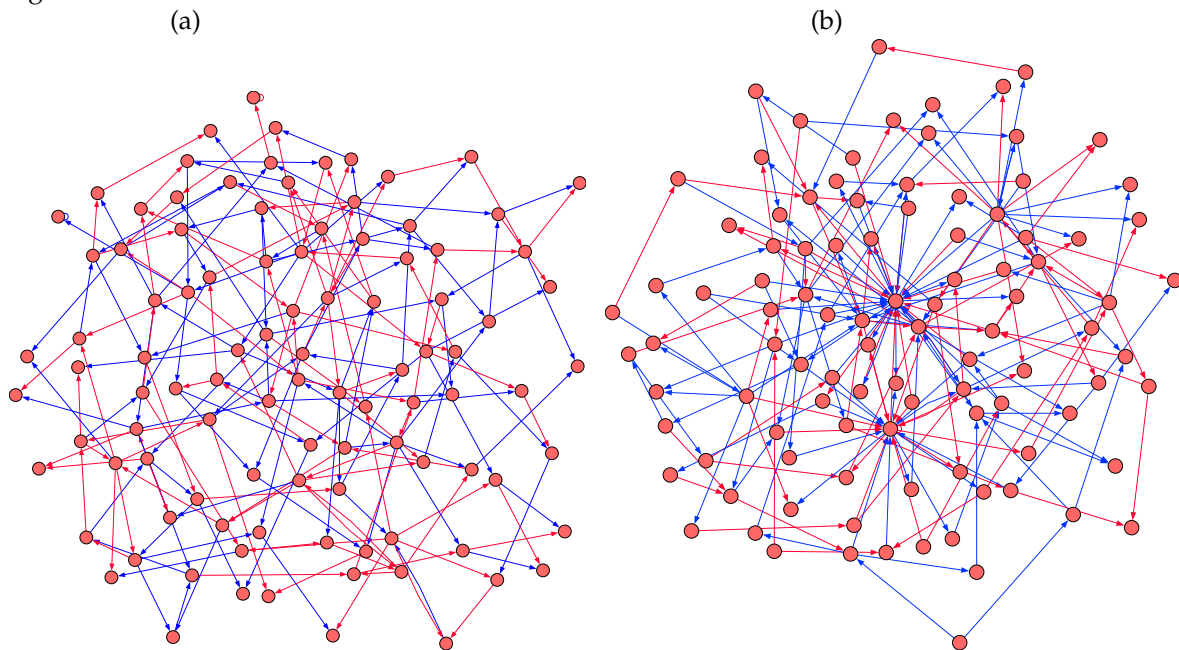


Figure 8.

